NASA Contractor Report 178175

ICASE REPORT NO. 86-59

ICASE

FINITE LENGTH EFFECTS IN TAYLOR-COUETTE FLOW

C. L. Streett

M. Y. Hussaini

Contract Nos. NAS1-17070, NAS1-18107

September 1986

INSTITUTE FOR COMPUTER APPLICATIONS IN SCIENCE AND ENGINEERING
NASA Langley Research Center, Hampton, Virginia 23665

Operated by the Universities Space Research Association

National Aeronautics and
Space Administration

Langley Research Center
Hampton, Virginia 23665

FINITE LENGTH TAYLOR COUETTE FLOW

C. L. Streett

NASA Langley Research Center, Hampton, Virginia 23665-5225

M. Y. Hussaini

Institute for Computer Applications in Science and Engineering

NASA Langley Research Center, Hampton, Virginia 23665-5225

Abstract

Axisymmetric numerical solutions of the unsteady Navier-Stokes equations for flow between concentric rotating cylinders of finite length are obtained by a spectral collocation method. These representative results pertain to two-cell/one-cell exchange process, and are compared with recent experiments.

Research was supported by the National Aeronautics and Space Administration under NASA Contract Nos. NAS1-17070 and NAS1-18107.

Introduction

The Taylor experiment on Couette flow between coaxial circular cylinders has been the subject of numerous theoretical and experimental studies [1]. This flow is rich in complex phenomena; so rich, in fact, that they are still being discovered [2], and our understanding of them is far from complete. In a typical Taylor experiment, the inner cylinder rotates with a constant angular velocity while the outer cylinder, along with the top and bottom walls, are kept at rest. The relevant geometric parameters are the radius ratio, which is the ratio of the radii of the inner and outer cylinders , and the aspect ratio, which is the ratio of the length of the annulus to its width. The dynamic parameter is the Reynolds number based on the angular velocity of the inner cylinder and the annulus width. The Taylor-Couette flow is strongly dependent on all of these parameters. The theory for the infinite aspect ratio case (which neglects end wall effects) and its correspondence to the experiments in cylinders of necessarily finite but large aspect ratio are reviewed in Di Prima and Swinney [1] and Di Prima [3]. Benjamin [4] has developed a rigorous qualitative theory for the existence of nonunique steady states for confined flows and their stability and transition with particular reference to finite-length Taylor-Couette flow. His predictions have been confirmed in a series of experiments [5] in cylinders of short length with fixed end plates. They have been further confirmed by the numerical results of Cliffe and Mullin [6] who discretized the steady Navier Stokes equations by a Galerkin finite element method and solved the resulting nonlinear algebraic equations by the pseudo arclength continuation method of Keller [7].

Among other numerical studies of the finite-length Taylor-Couette flow problem, those of Alziary de Roquefort and Grillaud [8], and Neitzel [9] are

worth mentioning. Both investigations were based on the time dependent vorticity-stream function formulation along with the equation for the azimuthal velocity. They used a finite difference method to solve for the steady state by a time asymptotic approach. Their numerical results show the axial structure for small Reynolds number, the smooth development of the flow with rapid increase in vortex activity for Reynolds numbers in quasi-critical range, and multiple states for sufficiently large Reynolds number. The aspect ratio being large, their results are only pertinent to the exchange phenomena beyond the two-cell and four-cell interactions examined by Benjamin.

No theoretical work on finite-length Taylor-Couette flow has incorporated the correct boundary conditions for fixed end walls. An idealized version of the end-wall boundary conditions is due to Schaeffer [10]. He introduces a parameter alpha in the boundary conditions, with $0 < \alpha < 1$. The parameter α interpolates linearly between the two extreme cases: $\alpha = 0$ corresponds to the infinite length problem which accommodates the Couette flow as an exact solution, while $\alpha = 1$ corresponds to the finite length problem with the correct no-slip conditions being applied on the end walls.

For $\alpha = 0$, Blennerhasset and Hall [11] have considered the linear stability problem in the small gap limit, and the key result was that the two-cell primary flow changes into four-cell at the aspect ratio of approximately 2.6. This should be compared with a value of roughly 3.7 observed by Benjamin for radius ratio of 0.615. Hall [12] has further derived the amplitude equations for this problem. An interesting feature of these amplitude equations is a quadratic term (absent in the infinite aspect ratio case) which can introduce hysteresis and soften bifurcations into smooth transitions.

For small nonzero values of α , Schaeffer [10] used a Lyapunov-Schmidt reduction procedure and the methods of singularity theory to obtain results applicable to the exchange processes between 2m and 2m+2 cells, $m > 2$. Hall [12] has studied the two cell-four cell exchange problem using amplitude equations and a perturbation method for small values of alpha.

The purpose of our continuing research effort is to solve the unsteady Navier-Stokes equations by a highly accurate spectral collocation method with a view to elucidate the underlying processes leading to laminar-turbulent transition in the Taylor-Couette flow. The present work is confined to the evolution of two-cell and single-cell Taylor-Couette flows with specific reference to the experiments of Benjamin and Mullin [13], Lucke, et al. [14] and Aitta, et al [15]. The main result of these studies is a second order transition from a two-cell flow, symmetric under reflection about the mid-plane, to an asymmetric single-cell flow that ensues with increasing Reynolds number beyond a certain critical value.

Splitting Scheme

The incompressible Navier-Stokes equations for axisymmetric flow in a cylindrical geometry are, in conservation form:

$$\frac{\partial u}{\partial t} + \frac{\partial (u^2)}{\partial r} + \frac{\partial (uw)}{\partial y} + \frac{(u^2 - v^2)}{r} = - \frac{\partial P}{\partial r} + \nu [\nabla^2 u - \frac{u}{r}] \qquad (1)$$

$$\frac{\partial v}{\partial t} + \frac{\partial (uv)}{\partial r} + \frac{\partial (vw)}{\partial y} + \frac{2uv}{r} = \nu [\nabla^2 v - \frac{v}{r}] \qquad (2)$$

$$\frac{\partial w}{\partial t} + \frac{\partial (uw)}{\partial r} + \frac{\partial (w^2)}{\partial y} + \frac{uw}{r} = \frac{\partial P}{\partial y} + \nu \nabla^2 w \qquad (3)$$

$$\frac{1}{r}\frac{\partial}{\partial r}(ru) + \frac{\partial w}{\partial y} = 0$$

$$\text{where } \nabla^2 \equiv \frac{1}{r}\frac{\partial}{\partial r}\left(r\frac{\partial}{\partial r}\right) + \frac{\partial^2}{\partial y^2} \tag{4}$$

and u, v, w are the r, θ and y components of velocity, respectively. For the case where the outer cylinder and end plates are stationary, and the inner cylinder rotates, the boundary conditions are:

$u = v = w = 0$ on the outer cylinder $r = R_o$,

and at the top and bottom wall $y = \pm y_\ell$

$u = w = 0$ on the inner cylinder $r = R_i$

$v = \Omega R_i$.

In the present calculations, the azimuthal velocity v is split into two parts, $v = v_b + \tilde{v}$, where v_b satisfies:

$$\nabla^2 v_b = 0$$

$$v_b = 0 \text{ at } r = R_o, \text{ and at } y = \pm y_\ell$$

$$= \Omega R_i \text{ at } r = R_i$$

The quantity v_b is computed and stored at the start of a calculation, which proceeds with the computation of u, $\tilde{v}$, and w at each time step. Note that these three velocity components satisfy homogeneous boundary conditions.

A splitting method is employed to advance the solution from t^n to t^{n+1}. Writing the Navier-Stokes equations in vector notation with $\underline{u}$ representing the velocity, $(u, \tilde{v}, w)$, we have:

$$\underline{u}_t + \underline{u}\cdot\nabla\underline{u} = -\nabla P + \nu\nabla^2\underline{u} \quad \text{in D, the annulus} \tag{5}$$

$$\nabla\cdot\underline{u} = 0$$

$$\underline{u} = 0 \text{ on the boundary } \Gamma$$

the split scheme first advances $\underline{u}^n$ to an intermediate solution $\underline{u}^*$ by solving:

$$\underline{u}^*_t + \underline{u}^*\cdot\nabla\underline{u}^* = \nu\nabla^2\underline{u}^* \tag{6}$$

$$\underline{u}^* = \underline{g}^* \text{ on } \Gamma.$$

The intermediate boundary condition $\underline{u}^* = \underline{g}^*$ will be discussed subsequently. Finally, the solution is advanced from $\underline{u}^*$ to $\underline{u}^{n+1}$ via:

$$\underline{u}^{n+1}_t = -\nabla P^{n+1}$$

$$\nabla\cdot\underline{u}^{n+1} = 0 \tag{7}$$

$$\hat{n}\cdot\underline{u}^{n+1} = 0 \quad \text{on } \Gamma$$

where $\hat{n}$ is unit normal to the boundary Γ. Note that the final, "pressure correction" step by itself is an inviscid calculation, and is well-posed when only boundary conditions on the normal component of velocity are enforced. At the end of the full step there exists a non-zero tangential component of velocity on the boundary. The magnitude of this slip velocity can be reduced

by a proper choice of the intermediate boundary condition on $\underline{u}^*$. Marcus [16] has described the difficulties which arise from the use of $\underline{u}^* = 0$ as the intermediate boundary condition. The conditions used here are based on the work of Fortin, et al. [17]. Using backward Euler time discretization for Eq. 7 yields:

$$u^{n+1} = u^* - \Delta t \, \nabla P \tag{8}$$

and the slip velocity on the boundary is given by

$$\hat{\tau} \cdot \underline{u}^{n+1}|_\Gamma = \hat{\tau} \cdot (\underline{u}^*|_\Gamma - \Delta t \, \nabla P^{n+1}|_\Gamma) \tag{9}$$

If $\hat{\tau} \cdot \underline{u}^* = 0$ on the boundary, then $\hat{\tau} \cdot \underline{u}^{n+1}|_\Gamma = 0(\Delta t)$ where $\hat{\tau}$ is the unit tangent to the boundary Γ. However, if ∇P^{n+1} is expanded in Taylor series about $t = t^n$:

$$\nabla P^{n+1} = \nabla P^n + \Delta t \, \nabla P_t^n + 0(\Delta t^2)$$

and the second term is approximated by

$$\Delta t \, \nabla P_t^n = (\nabla P^n - \nabla P^{n-1}) + 0(\Delta t^2)$$

then Eq. 8 becomes

$$\hat{\tau} \cdot \underline{u}^{n+1}|_\Gamma = \hat{\tau} \cdot \underline{u}^*|_\Gamma - \Delta t \, (2\nabla P^n - \nabla P^{n-1}) + 0(\Delta t^3).$$

Thus the slip velocity may be reduced to $O(\Delta t^3)$ through the intermediate boundary condition

$$\hat{\tau} \cdot \underline{u}^*|_\Gamma = \hat{\tau} \cdot \Delta t \, (2\nabla P^n - \nabla P^{n-1}). \tag{10}$$

Of course the boundary condition $\hat{n} \cdot \underline{u}^* = 0$ is retained.

The pressure step is actually carried out in two parts. First, the divergence of the first of Eqs. 8 yields:

$$\nabla^2 P^{n+1} = \frac{1}{\Delta t} \nabla \cdot \underline{u}^* \tag{11}$$

where $\nabla \cdot \underline{u}^{n+1} = 0$ is enforced. Then the velocities are updated using

$$\underline{u}^{n+1} = u^* - \Delta t \, \nabla P^{n+1} \tag{12}$$

Note that this formulation requires a boundary condition for the pressure. This poses a problem, since there is no natural boundary condition for pressure. Deriving a condition by enforcing the normal momentum equation at the boundary is a questionable practice, as the equation need not hold on the boundary at the differential level of the equations. This inconsistency often produces explosive instability in a spectral code. Fortunately, the split scheme yields a self-consistent pressure condition,

$$\hat{n} \cdot \nabla P|_\Gamma = 0 \tag{13}$$

since both $\hat{n} \cdot \underline{u}^*$ and $\hat{n} \cdot \underline{u}^{n+1}$ are zero on the boundary. The error involved

in this specification is, we believe, related to the overall splitting error of the scheme.

Zang and Hussaini [18], have extensively investigated a related split scheme in which two coordinate directions were periodic and the third employed general boundary conditions. Comparison between split and unsplit codes using the same discretization yielded agreement to five decimal digits. However, they utilized a staggered grid for pressure in the non-periodic direction, obviating the need for a pressure boundary condition. Staggered grids in two dimensions either lack the ability to set both velocity components equal to zero on all boundaries, or are susceptible to an oscillatory "checkerboard" pressure mode. The unstaggered scheme used here, on the other hand, requires a pressure boundary condition. Actually, the consistent pressure equation derived by Zang and Hussaini yields exactly the same condition on pressure as used here. No instabilities were ever encountered with the present scheme.

Discretization and Solution Scheme

Since no-slip boundary conditions are enforced in both the r and y directions, Chebyshev spectral representation is appropriate in both directions. Collocation is used for a number of reasons: straightforward treatment of nonlinear terms and boundary conditions; capability to include coordinate stretchings; and ability to solve the resulting discrete equations rapidly. For further discussion of this form of discretization, see Hussaini et al. [11].

A coordinate stretching was employed in the radial direction to resolve the large gradients near the inner cylinder. The form of the stretching is:

$$r = \frac{[1 + b \exp(-a)]\,(R_o - R_i)}{[1 + b \exp(-a\, r_c)]}\; r_c + R_i \tag{14}$$

where r_c is the radial coordinate in the computational space. Values of a = 2 and b = 5 to 50 were typical in this work. The y-direction was not stretched.

Time discretization of the first step in the split scheme involved the low-storage mixed Runge-Kutta/Crank-Nicholson scheme [20]. Writing the semi-discrete equation for the first step as

$$u_t = A(u) + D(u) \tag{15}$$

where A(u) and D(u) represent advection and diffusion terms, respectively, the mixed scheme advances from time step t^n to t^{n+1} using a third-order Runge-Kutta scheme for the advection terms and Crank-Nicholson for the diffusion terms:

$$\begin{aligned}
u^0 &= u(t^n) \\
H^1 &= \Delta t\, A(u^0) \\
u^1 &= u^0 + \tfrac{1}{3} H^1 + \tfrac{1}{6} \Delta t\, (D(u^0) + D(u^1)) \\
H^2 &= \Delta t\, A(u^1) - \tfrac{5}{9} H^1 \\
u^2 &= u^1 + \tfrac{15}{16} H^2 + \tfrac{5}{24} \Delta t\, (D(u^1) + D(u^2)) \\
H^3 &= \Delta t\, A(u^2) - \tfrac{153}{128} H^2 \\
u^3 &= u^2 + \tfrac{8}{15} H^3 + \tfrac{1}{8} \Delta t\, (D(u^2) + D(u^3))
\end{aligned} \tag{16}$$

$$u\ (t^{n+1}) = u^3$$

The second step of the split scheme uses backward Euler time discretization, as mentioned in the previous section.

The above scheme is stable to O(1) Courant numbers, which involves time steps many times larger than that desired for accuracy. Typically a time step which resulted in Courant numbers of .1 to .2 based on the smallest physical mesh spacing was used. The slip velocity resulting from the choice of time step was normally eight to ten orders of magnitude below the maximum velocity in a given direction.

Note that the above scheme reduces the problem to a sequence of uncoupled Helmholtz/Poisson equations to advance the discrete solution. Since one time step requires the solution of nine positive-definite Helmholtz equations with Dirichlet boundary conditions, and one Poisson equation with pure Neumann boundary conditions, a computationally efficient technique had to be developed if this study is to be feasible. The present scheme is fairly efficient. This scheme involves preconditioned Richardson iteration, in which an optimum relaxation parameter is chosen dynamically using a principle of either minimum-residual (MR) or orthogonal-residual (OR) procedure. Details of this technique are as follows.

Write the equation to be solved as

$$L(u) = f \tag{17}$$

The residual at a given iterate "m" is

$$R^m \equiv L(u^m) - f \tag{18}$$

A preconditioned iteration scheme may be looked at in the following way. At a given iteration, the goal is to compute an update such that the next residual is zero, i.e.

$$R^{m+1} \equiv L(u^m + \Delta\tilde{u}) = 0 \tag{19}$$

or for a linear operator L (as in this case):

$$L(u^m) + L(\Delta\tilde{u}) = R^m + L(\Delta\tilde{u}) = 0 \tag{20}$$

Approximating the operator L which is difficult to invert by a more easily-inverted operator M yields the following preconditioned scheme for the update:

$$\Delta\tilde{u} = M^{-1}[L(u^m)] = M^{-1}[R^m] \tag{21}$$

A well-known method for computing an optimal ω^m involves minimizing the L_2 norm of the residual, R^{m+1}:

$$\begin{aligned} \min_{\omega^m} (R^{m+1}, R^{m+1}) &= \min_{\omega^m} (R^m, R^m) = 2\omega^m (R^m, L(\Delta\tilde{u})) \\ &\quad + \omega^{m^2} (L(\Delta\tilde{u}), L(\Delta\tilde{u})) \end{aligned} \tag{22}$$

for which a stationary point is

$$\omega^m = - \frac{(R^m, L(\Delta\tilde{u}))}{(L(\Delta\tilde{u}), L(\Delta\tilde{u}))} \tag{23}$$

This is the usual minimum residual (MR) method.

An alternate method for chosing ω^m is to require that the successive residuals be orthogonal to each other. This yields an orthogonal residual (OR) scheme related to the method of steepest descent:

$$(R^m, R^{m+1}) = (R^m, R^m) + \omega^m (R^m, L(\Delta\tilde{u})) = 0 \tag{24}$$

and hence

$$\omega^m = - \frac{(R^m, R^m)}{(R^m, L(\Delta\tilde{u}))} \tag{25}$$

The scheme proceeds as follows from an initial guess u^0 and residual $R^0 = L(u^0) - f$:

$$\Delta\tilde{u} = M^{-1} [R^m]$$

$$u^{m+1} = u^m + \omega^m \Delta\tilde{u} \tag{26}$$

$$R^{m+1} = R^m - \omega^m L(\Delta\tilde{u})$$

etc.

The preconditioning operator M is the second-order finite-difference operator which corresponds to the spectral operator L. Unequal-mesh spacing formulae, based on the physical-space point locations (which includes the radial stretching), are used in constructing M. A fixed V-cycle multigrid scheme driven by approximate-factorization is used to invert the preconditioning operator (Eq 21). It was found that complete convergence of

this step is not required for the overall preconditioned scheme to converge: essentially no difference in convergence rate is seen between fully solving the preconditioning step and merely reducing the residual (associated with inversion of the preconditioner) by two orders of magnitude which usually requires only two or three multigrid cycles.

The overall convergence rate based on spectral operator evaluations is never slower than .35 (for Dirichlet boundary conditions); rates between .15 and .2 are typical even on the highly stretched mesh. The use of MR or OR to compute the optimum relaxation factor yields equivalent convergence rates, although the OR scheme is found to be more robust in other contexts.

However, the observed convergence rate deteriorates for this scheme when it is applied to the pure Neumann problem encountered in the Eqs (11) and (13). Since a large number of such problems are to be solved, a boundary influence-matrix technique is devised that reduces the computation time associated with this step. To compute the solution of

$$\begin{aligned} L(u) &= f \text{ in } D \\ u_n &= 0 \text{ on } \Gamma \end{aligned} \tag{27}$$

a series of homogeneous solutions $u^{(i)}$ is obtained:

$$\begin{aligned} L(u^{(i)}) &= 0 \text{ in } D \\ u^{(i)} &= \delta(x_i) \text{ on } \Gamma \end{aligned} \tag{28}$$

for each boundary point x_i. For each solution $u^{(i)}$, , the vector of normal gradients $[u_n^{(i)}]$ at all boundary points is computed. These vectors are collected as columns of a (square) matrix. This matrix is the influence of a unit disturbance at the boundary on the normal gradient at the boundary of the solution to the linear operator $L(u) = 0$. Denote this matrix by

$$C = \text{col} \{[u_n^{(1)}], [u_n^{(2)}], \ldots [u_n^{(N_b)}]\} \tag{29}$$

where a total of N_b points lie on the boundary. The matrix C may be inverted to yield the influence of a unit normal gradient at the boundary on the boundary value of a solution of $L(u) = 0$, with provision for setting the level of the solution required. Then the solution of the original problem (Eq. 27) proceeds by solving the related problem with homogeneous Dirichlet boundary conditions:

$$\begin{aligned} L(u^h) &= f \quad \text{in} \quad D \\ u^h &= 0 \quad \text{on} \quad \Gamma \end{aligned} \tag{30}$$

The vector of normal derivatives of u^h at the boundary $[u_n^h]$ is computed. u^h must be corrected if it is to satisfy the desired Neumann boundary conditions. This correction is computed by applying the influence matrix to the boundary gradient error vector:

$$L(u^c) = 0 \text{ in } D$$

$$u^c = C^{-1}\,[u_n^h] \text{ on } \Gamma \tag{31}$$

The desired solution is $u = u^h + u^c$.

Computation and inversion of the influence matrix is done in a preprocessing step; since it is a function only of the mesh geometry, it may be stored and used whenever it is needed. To obtain a solution of the pure Neumann-Poisson problem at each time step requires that we solve just two Dirichlet-Poisson problems and the solutions satisfy the desired boundary conditions exactly.

Implementation and Performance:

The above split scheme for solving the time-dependent incompressible Navier-Stokes equations has been inplemented with a view to processing on both scalar and vector computers. In scalar form on a CYBER-175, the code requires approximately 20 seconds per time step on a 17 x 17 mesh, and 56 seconds/step on a 25 x 25 mesh. A large fraction of these times is spent in computing the 11 Helmholtz/Poisson solutions required in each time step. On the VPS-32 vector processing machine at NASA Langley, the vector code requires about 14 seconds step on a mesh comprised of 65 points in the y direction and 33 points in the r direction. Almost 85 percent of this time is taken in inverting the preconditioning step of the Helmholtz/Poisson solution as the approximate factorization part of the step is not vectorizable in a manner which yields adequate vector lengths for the two-dimensional problems. This observed performance for the two-dimensional Chebyshev-Chebyshev code is in line with

the performance quoted in (21) for a three-dimensional Chebyshev-Fourier-Fourier code (both codes have similar operation counts). For a coordinate direction discretized with Chebyshev series using N points, the operation count for that direction is $O(N^2)$, whereas a Fourier-discretized direction requires only O(N) operations. Thus, the present Chebyshev-Chebyshev method and the Chebyshev-Fourier-Fourier method both have total operation counts of $O(N^4)$, with the latter method having the advantage of larger possible vector lengths.

When the azimuthal direction is added to this simulation, however, the relative performance improves dramatically. Since the azimuthal direction is periodic, Fourier series is an appropriate discretization. The computations are performed in the Fourier wave-space of that direction; the discrete equations for each azimuthal mode decouple (see [21] for details)), allowing vector lengths to increase by a factor of the number of points in the azimuthal direction. This increase in vector length improves the CPU seconds/point/time step performance of the present scheme by a factor of four, and should allow the planned three-dimensional simulations to be performed.

RESULTS

The results presented here pertain to the axisymmetric two-cell/one-cell bifurcation, which occurs when the Taylor apparatus has an aspect ratio up to about 1.5. The form of the bifurcation depends sensitively on this parameter; experiments [15] show that this transition can change from supercritical to subcritical with variations in the aspect ratio of as little as eight percent.

Most of the results are obtained either by making quasi-static changes in the Reynolds number and allowing the stable, dominant mode to settle, or by slowly sweeping through a Reynolds number range, monitoring the change in a particular mode. Of course, using a time-accurate code to simulate the bifurcations of steady-state solutions is quite inefficient, owing to the extremely small growth rates near the bifurcation points. However, the eventual aim of this work is to simulate the turbulence and broadband structure exhibited by Taylor-Couette flow at moderate Reynolds numbers and the code was developed with these time dependent flows in mind. The ability to simulate accurately the sensitive, steady state bifurcations at lower Reynolds numbers is an excellent test for the numerical method.

Moreover, by using a time-dependent computation to investigate the steady state bifurcations, we can obtain information on the path which the system follows as states exchange stability. This is illustrated by the following result. A 17 x 17 grid is used in all these simulations with a few calculations on a 25 x 25 mesh for accuracy check. The time step in these simulations corresponds to a maximum Courant number of about 0.2; the time step is limited by accuracy, and not by stability. For the geometry of Benjamin and Mullin [13] with a radius ratio .615, and aspect ratio 1.05, the symmetric two-cell mode is allowed to stabilize at a relatively low Reynolds number (R = 62). The Reynolds number is then raised impulsively to 165, above the experimental bifurcation boundary of about 150 and the growth of the one-cell asymmetric mode is observed. Random machine roundoff error on the order of 10^{-14} provides the initial energy for the mode. The order parameter used here to quantify the asymmetry of the mode is due to Lucke et al. [14]:

$$\psi = \frac{\int dr dz\ (u(r,z) - u(r,-z))}{\int dr dz\ (|u(r,z)| + |u(r,-z)|)}$$

The integrals were performed by spectral collocation. The logarithm of this parameter is shown in Fig. 1 plotted against time in units of the diffusion time scale y_ℓ^2/ν. As can be seen, the initial instability leading to the one-cell mode appears to be linear; that is, exponential growth with time is observed with only the later stages being modulated by nonlinear effects. Also shown in Fig. 1 is a plot of the logarithm of the disturbance energy versus time. After an initial period, the disturbance energy grows at a rate which is within 2% of double the growth rate of ψ as expected.

Streamlines in a cross-sectional plane at various stages in the two-cell/one-cell exchange are shown in Fig. 2. Locations of these intermediate states on the ψ vs time curve are indicated in Fig. 1. Note that the progression between states is smooth without abrupt collapse or alteration of the flowfield structure.

The geometry of Lucke, et al. [14] has a radius ratio of .5066, and an aspect ratio of 1.05. This choice of parameters leads to a smooth supercritical bifurcation to the one-cell mode as the Reynolds number is increased beyond a critical value. A plot of the order parameter against Reynolds number for this simulation is shown in Fig. 3. This curve is traced in the direction of both increasing and decreasing Reynolds number. As we approach the initial critical value, the Reynolds number is varied very slowly at a rate of about $\pm$ .2 units based on the diffusion time scale. The growth rates are much larger on the upper branch of this plot, which permits larger changes in Reynolds number. This bifurcation diagram is validated by

restarting the simulation at various points along the curve and allowing the flow to settle to eight decimal digits for a fixed Reynolds number.

Also shown in Fig. 3 are the results of Lucke et al. [14] for this case. Their results were computed using a staggered-grid finite-difference scheme on a grid of about 28 x 30 points; however, in that calculation the Reynolds number was changed at a rate of about 4.1 based on the present time scale. A large discrepancy in the critical Reynolds number as predicted by these two studies is noted.

We also investigated the geometry of Aitta, et al. [15] where the radius ratio is .5. Their experimental results relate to three aspect ratios: 1.129, 1.266, and 1.281; for which the two-cell/one-cell bifurcations are supercritical, transcritical, and subcritical, respectively. In Fig. 4, an order parameter due to Aitta et al. [15] is plotted as a function of Reynolds number.

$$\psi' = \frac{\int_{-y_\ell}^{+y_\ell} w(r,y)\, dy}{\int_{-y_\ell}^{+y_\ell} |w(r,y)|\, dy}$$

where $r = R_i + .14(R_o - R_i)$. Also shown in Fig. 4, are the experimental results of Aitta, et al. The two loci of states agree in form. They also agree as to the level at which the asymmetric branch becomes unstable and the width of the region in which both symmetric and asymmetric modes are stable. The critical Reynolds number from the simulation is within 3% of that of the experiment. The growth rates of the one-cell mode in the "hysteresis" region of the bifurcation are exceedingly small, several orders of magnitude below

those observed in the first two cases, producing a flow costly to simulate accurately. Resolution requirements are also large; a 33 x 33 mesh is required for this simulation.

References

[1] DiPrima, R. C. and H. L. Swinney, "Instabilities and transitions in flow between concentric rotating cylinders," Hydrodynamic Instabilities and the Transition to Turbulence, H. L. Swinney and J. P. Gollub (eds.), Springer-Verlag, New York 1981.

[2] Pfister, G., "Deterministic chaos in rotational Taylor-Couette flow," Lecture Notes in Physics, No. 235, pp. 199-210, 1985.

[3] DiPrima, R. C., "Transition in flow between rotating concentric cylinders," Transition and Turbulence. R. E. Meyer (ed.), Academic Press, 1981.

[4] Benjamin, T. B., "Bifurcation phenomena in steady flow of a viscous fluid I. Theory." Proc. R. Soc. London A 359, 1-26, 1978.

[5] Benjamin, T. B., "Bifurcation phenomena in steady flows of a viscous fluid II. Experiments." Proc. R. Soc. London A 359, 27-43, 1978.

[6] Cliffe, K. A. and T. Mullin, "A numerical and experimental study of anomalous modes in the Taylor experiment." J. Fluid Mech., 1985, vol 153, pp. 243-258.

[7] Keller, H. B., "Numerical solutions of bifurcation and nonlinear eigenvalue problems." Applications of Bifurcation Theory, (ed. P. H. Rabinowitz), pp. 359-384, Academic Press.

[8] Alziary de Roquefort, T., G. Grillaud, "Computation of Taylor vortex flow by a transient implicit method." Comput. Fluids 6, 259-269, 1978.

[9] Neitzel, G. P., "Numerical computation of time-depenent Taylor-vortex flows in finite length geometries." J. Fluid Mech., 1984, vol. 141, pp. 51-66.

[10] Schaeffer, D. G., "Qualitative analysis of a model for boundary effects in the Taylor problem." Math Proc. Camb. Philos. Soc. 87, 307-337 (1980).

[11] Blennerhasset, P. J., P. Hall, "Centrifugal instabilities of circumferential flow in finite cylinders: linear theory." Proc. R. Soc. London A 365, 191-207 (1979).

[12] Hall, P., "Centrifugal instabilities in finite containers: a periodic model." J. Fluid Mech., 1980, vol. 99, pp. 575-596.

[13] Benjamin, T. B. and T. Mullin, "Anomalous modes in the Taylor experiment." Proc. Roy. Soc. London A 377, 221-249, 1981.

[14] Lucke, M., M. Mihelcic, K. Wingerath, and G. Pfister, "Flow in a small annulus between concentric cylinders." J. Fluid Mech., vol 140, pp. 343-353, 1984.

[15] Aitta, A., G. Ahlers, and D. S. Cannel, "Tricritical phenomena in rotating Couette-Taylor flow." Phys. Rev. Lett., vol 54, pp. 673-676, 1985.

[16] Marcus, P., "Simulation of Taylor-Couette flow - numerical methods and comparison with experiment." J. Fluid Mech., vol 146, pp. 45-64, 1984.

[17] Fortin, M., R. Peyret, and R. Temam, "Resolution numerique des equations de Navier-Stokes pour un fluide incompressible." J. de Mecanique, vol 10, pp. 357-390, 1971.

[18] Zang, T. A. and M. Y. Hussaini, "On spectral multigrid methods for the time-dependent Navier-Stokes equations." Appl. Math. Comp., vol 19, pp. 359-372, 1986.

[19] Hussaini, M. Y., C. L. Streett, and T. A. Zang, "Spectral methods for partial differential equations." Proc. 1st Army Conf. on Appl. Math. and Computing, ARO Report 84-1, 1984.

[20] Williamson, J. H., "Low-storage Runge-Kutta schemes." J. Comp. Phys., vol 35, no. 1, March 1980, pp. 48-56.

[21] Zang, T. A. and M. Y. Hussaini, "Numerical experiments on subcritical transition mechanisms." AIAA Paper No. 85-0296, 1985.

$\Gamma = 1.05$

$\eta = .615$

$R = 150$

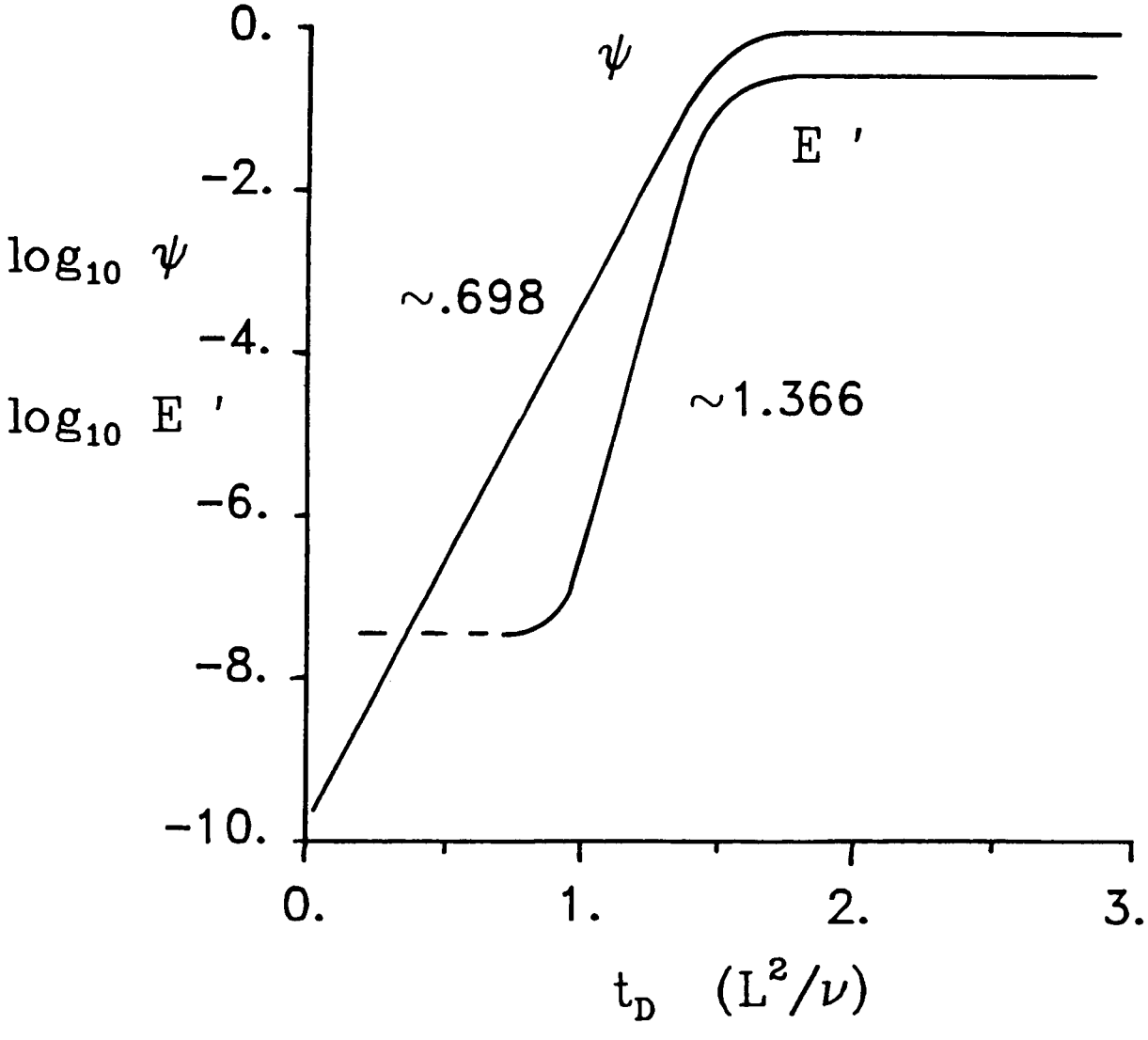

Figure 1

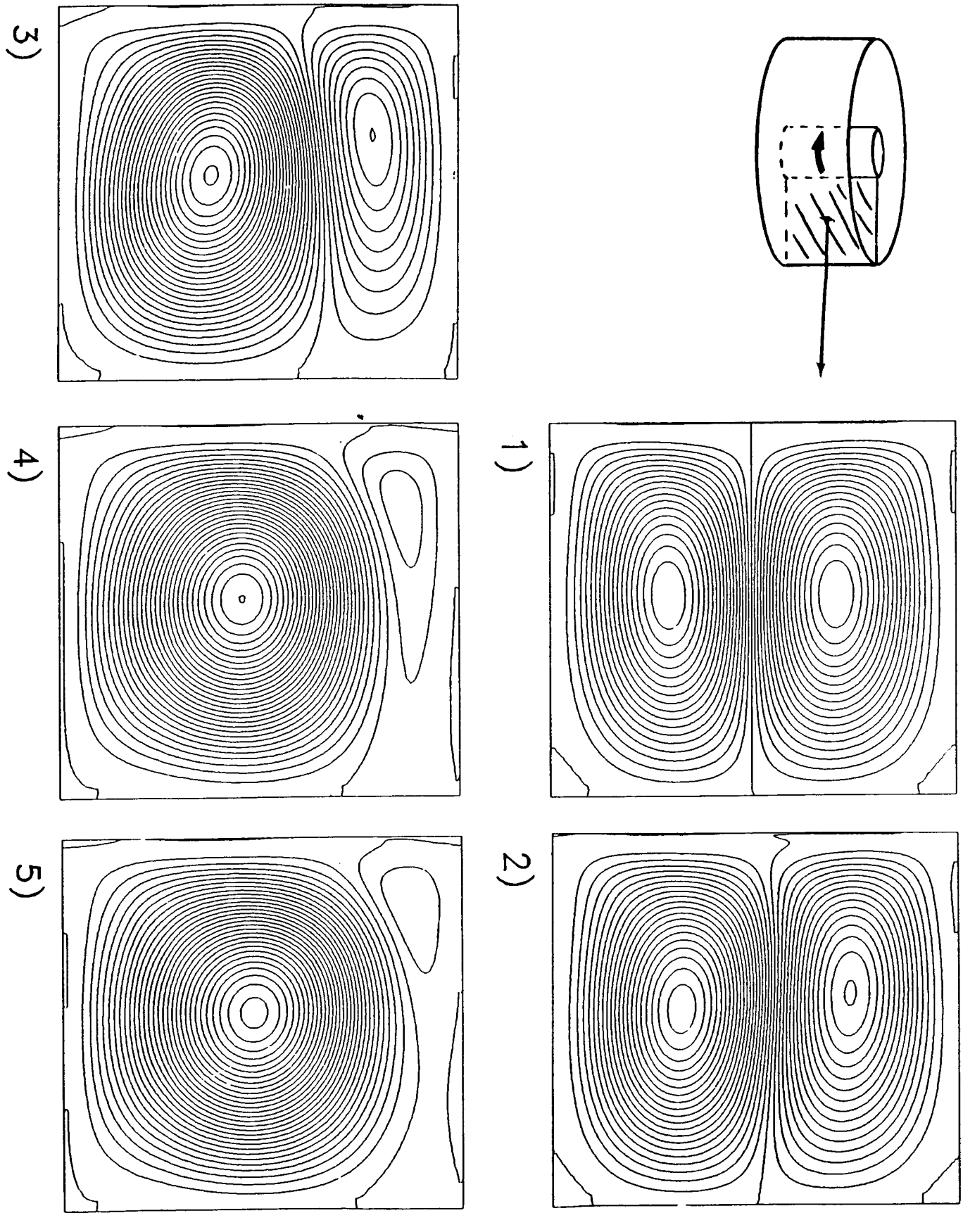

Figure 2

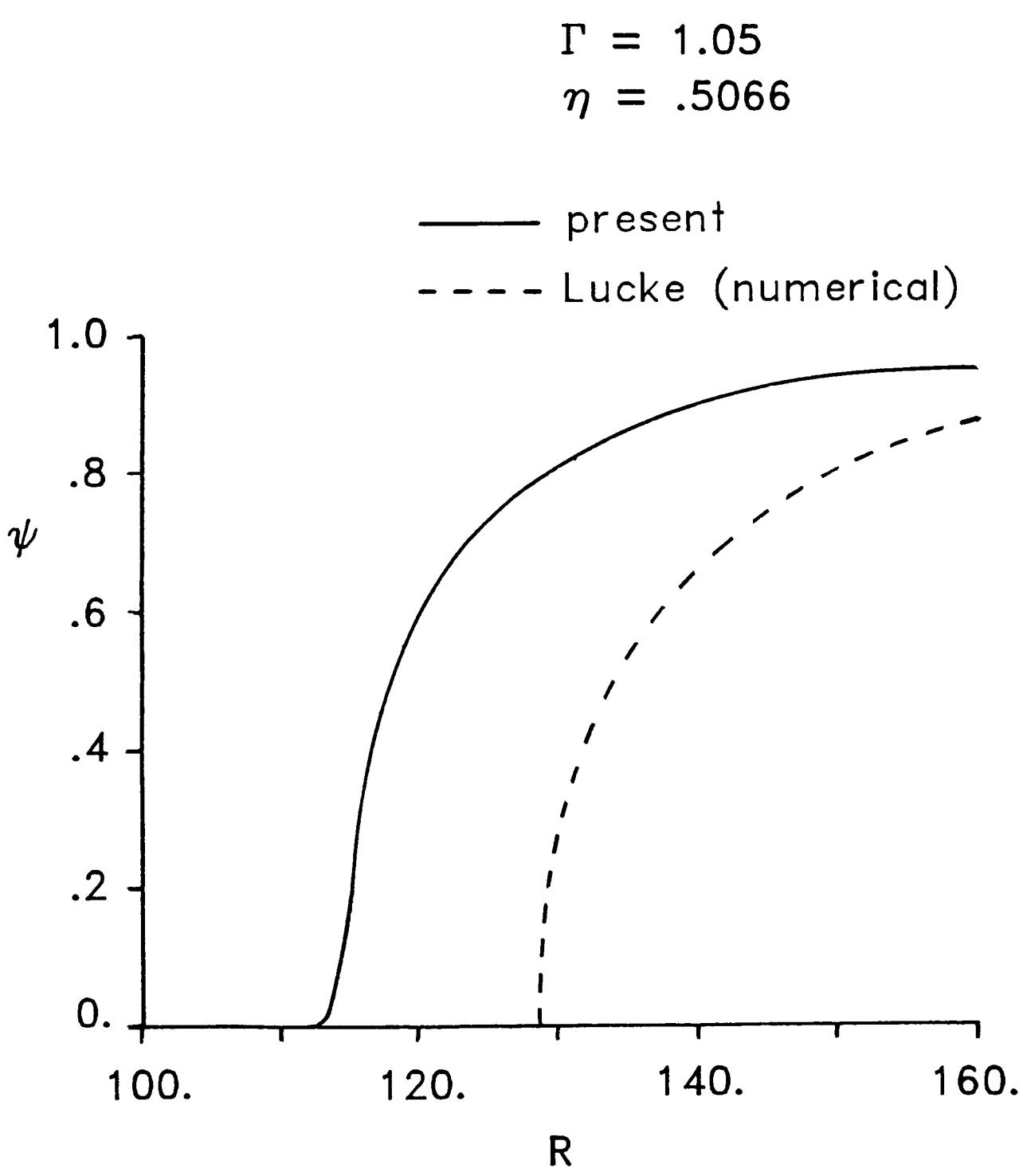
Γ = 1.05
η = .5066
present
Lucke (numerical)
1.0
.8
.6
.4
.2
0.
ψ
100.
120.
140.
160.
R

Figure 3

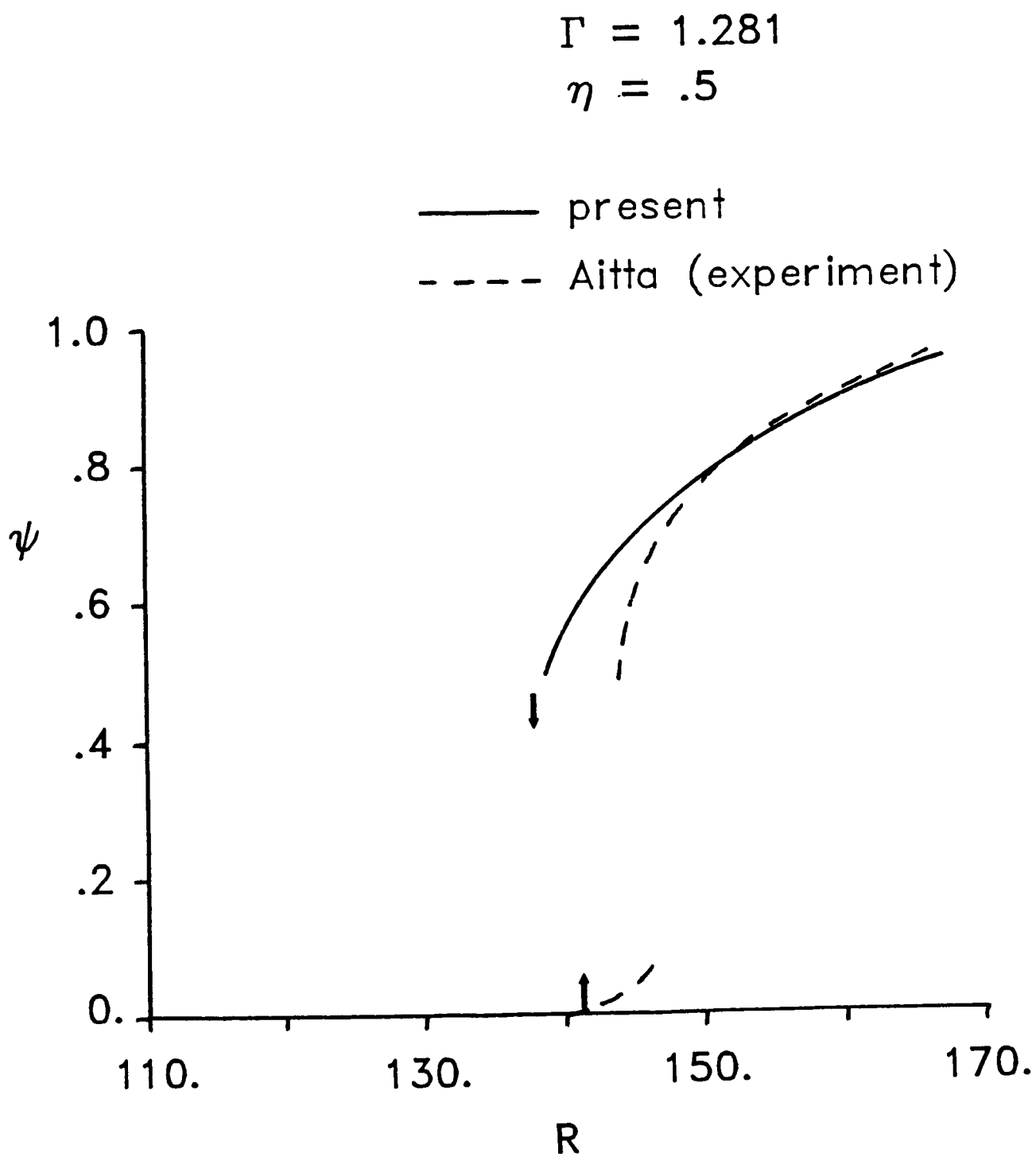
Γ = 1.281
η = .5
present
Aitta (experiment)
1.0
.8
.6
.4
.2
0.
ψ
110.
130.
150.
170.
R

Figure 4

Standard Bibliographic Page

1. Report No. NASA CR-178175 ICASE Report No. 86-59	2. Government Accession No.	3. Recipient's Catalog No.
4. Title and Subtitle FINITE LENGTH EFFECTS IN TAYLOR-COUETTE FLOW		5. Report Date September 1986 6. Performing Organization Code
7. Author(s) C. L. Streett and M. Y. Hussaini		8. Performing Organization Report No. 86-59
9. Performing Organization Name and Address Institute for Computer Applications in Science and Engineering Mail Stop 132C, NASA Langley Research Center Hampton, VA 23665-5225		10. Work Unit No. 11. Contract or Grant No. NAS1-17070, NAS1-18107
12. Sponsoring Agency Name and Address National Aeronautics and Space Administration Washington, D.C. 20546		13. Type of Report and Period Covered Contractor Report 14. Sponsoring Agency Code 505-90-21-01

15. Supplementary Notes

Langley Technical Monitor:
J. C. South

Final Report

Submitted to Proc. Workshop on "The Stability of Time-Dependent/ Spatially Varying Flows"

16. Abstract

Axisymmetric numerical solutions of the unsteady Navier-Stokes equations for flow between concentric rotating cylinders of finite length are obtained by a spectral collocation method. These representative results pertain to two-cell/one-cell exchange process, and are compared with recent experiments.

17. Key Words (Suggested by Authors(s))	18. Distribution Statement
bifurcation, two-cell/one-cell exchange, flow in concentric rotating cylinders	34 - Fluid Mechanics and Heat Transfer 64 - Numerical Analysis Unclassified - unlimited

19. Security Classif.(of this report)	20. Security Classif.(of this page)	21. No. of Pages	22. Price
Unclassified	Unclassified	30	A03

For sale by the National Technical Information Service, Springfield, Virginia 22161

NASA-Langley, 1986